Zirconium Alkoxides as Components of Hybrid Inorganic−Organic Macromolecular Materials†

R. Di Maggio,* L. Fambri, and A. Guerriero‡

Dip. di Ingegneria dei Materiali, Via Mesiano, 77, Dip. di Fisica, Via Sommarive Povo, Università degli Studi di Trento, 38050 Trento, Italy

Received October 22, 1997. Revised Manuscript Received April 28, 1998

Two types of inorganic−organic hybrid materials were prepared in a one-step process by mixing zirconium butoxide or propoxide and 2-hydroxyethyl methacrylate (HEMA) with or without benzoyl peroxide (BPO). The reaction of the alkoxides with HEMA was followed by IR, NMR, and DSC analyses, performed at different times after the mixing. NMR experiments suggest that free HEMA monomer is in fast exchange with that linked to zirconium ions. The mixtures containing BPO polymerized and stiffened in a few minutes after a mild thermal treatment. The hybrid materials are homogeneous and transparent, but brittle as well. Cerium(III) 2,4-pentanedionate was also added to modify the reactivity of zirconium alkoxides, and its role is invoked to account for the occurring free radical polymerization at room temperature. The formation of these HEMA−zirconia hybrid materials, showing glassy behavior and a remarkable thermal stability, is accompanied by low shrinkage.

Introduction

Due to their good refractory, mechanical, and optical properties, ZrO_2-based materials are used in a wide range of applications. Among these their application as protective films against corrosion on stainless steel by sol−gel process is particularly noteworthy.[1,2] However, it is difficult to obtain coatings thicker than 1 μm and monoliths by the conventional procedures, due to the high reactivity of the zirconium alkoxide precursors and the large shrinkage of the gels.

To overcome these problems, organic modifiers have been used to control the hydrolysis and condensation reactions and to improve the gel relaxation during the densification.[3−6] Moreover the modification of the inorganic backbones by organic groups has been recently studied as a way of forming stable and processable hybrid organic−inorganic composites. In most of hybrid materials already developed, the organic components are linked to the inorganic backbone[7−9] by Si−C covalent stable chemical bonds, leading to silicone type materials. Moreover, other reactions have been exploited. In fact an alternative route is represented by the synthesis of polyacrylate−silica composites from Si-$(OR)_4$ precursors, where R is a polymerizable group.[10] Some interesting studies were also found in the literature which use tetraethoxysilane (TEOS) along with vinyl polymer precursors. A polymeric network can be built up by the free-radical polymerization of the olefinic moieties (e.g. vinyl groups) of the organic monomer, along with the condensation of the inorganic compound.[11−15] As concerns zirconia-based polymers, they have been previously obtained from zirconium alkoxide precursors modified by selected ligands containing organic polymerizable functionalities.[16−18]

In this study, 2-hydroxyethyl methacrylate (HEMA), first polymerized by Wichterle and Lin,[19] was selected as an organic monomer in order to obtain zirconia-based hybrid materials, in which the organic polymer chains are uniformly distributed in, and directly linked to, the inorganic part, $Zr(OR)_4$ (R = Bu^n, Pr^n). A broad range of compositions was prepared by coupling the typical sol−gel reaction (e.g. hydrolysis and condensation) with the free radical polymerizazion. The Zr−OH groups, which quickly develop from the reaction of the zirconium

† This paper is dedicated to the memory of Prof. P. G. Orsini

* Corresponding author. E-mail: rosa.dimaggio@ing.unitn.it.

‡ Dip. di Fisica.

(1) De Lima Neto, P.; Atik, M.; Avaca, L.; Aegerter, M. A. *J. Sol-Gel Sci. Technol.* **1994**, *1*, 177.

(2) Di Maggio, R.; Fedrizzi, L.; Rossi S.; Scardi, P. *Thin Solid Films* **1996**, *286*, 127.

(3) Schmidt, H. *J. Sol-Gel Sci. Technol.* **1994**, *1*, 217.

(4) Debsidakar, J. C. *J. of Non-Cryst. Sol.* **1986**, *86*, 231.

(5) Chatry, M.; Henry, M.; In, M.; Sanchez, C.; Livage, J. *J. Sol-Gel Sci. Technol.* **1994**,*1*, 233.

(6) Chaibi, J.; Henry, M.; Zarrouk, H.; Gharbi N.; Livage, J. *J. Sol-Gel Sci. Technol* **1995**, *4*, 217.

(7) Philipp, G.; Schimdt, H. K. *J. Non-Cryst. Solids* **1984**, *63*, 283.

(8) Shea, K.; Loy, D. A. *Chem. Mater.* **1989**, *1*, 572.

(9) Schmidt, H. K. *Mater. Res. Soc. Symp. Proc.* **1991**, *180*, 961.

(10) Novak, B. M.; Davies, C. *Macromolecules* **1991**, *24*, 4, 5481.

(11) Wei, Y.; Wang, W.; Yang, D.; Tang, L. *Chem. Mater.* **1994**, *6*, 1737.

(12) Wojcik, A. B.; Klein, L. C. *J. Sol-Gel Sci. Technol.* **1995**, 5, 77.

(13) Yoshinaga, I.; Katayama, S. *J. Sol-Gel Sci. Technol.* **1996**, *6*, 151.

(14) Wei, Y.; Jin, D.; Yang, C.; Wei, G. *J. Sol-Gel Sci. Technol.* **1996**, *7*, 191.

(15) Wei, Y.; Jin, D. *Polym. Prepr. (Am. Chem. Soc., Div. Polym. Chem.)* **1997**, *38* (2), 122.

(16) Sanchez, C.; In, M. *J. Non-Cryst. Sol.* **1992**, *147 & 148*, 1.

(17) In, M.; Gerardin, C.; Lambard, J.; Sanchez, C. *J. Sol-Gel Sci. Technol.* **1995**, *5*, 101.

(18) Wei, Y.; Wand, W.; Yeh, J.-M.; Wang, B.; Yang, D.; Murray, J. K. Jr.; Jin, D.; Wei, G. *Hybrid Organic−Inorganic Composites*; Am. Chem. Soc. Symp. Ser. No 585; Mark, J. E., Lee, C. Y.-C., Bianconi, P. A., Eds.; American Chemical Society: Washington, DC, 1995; Chapter 11.

(19) Wichterle, O.; Lin, D. *Nature* **1960**, *185*, 177.

S0897-4756(97)00694-7 CCC: $15.00
Published on Web 06/13/1998

Table 1. Composition and Thermogravimetric Analysis of the Hybrid Materials, Obtained as Crack-Free Monoliths from Zirconium Alkoxides and 2-Hydroxyethyl Methacrylate (HEMA)

	ZBH14	ZBH12	ZBH11	ZPH14	ZPH12	ZPH11	ZBHM	ZPH	ZBH
r = [HEMA]/[Zr]	3.7	1.8	1	3.8	1.9	1	3.9	2	2
$Zr(OBu^n)_4$ (g)	3.17	4.23	4.99				2.53		4.12
$Zr(OPr^n)_4$ (g)				2.62	3.57	4.91		3.93	
HEMA (g)	3.34	2.31	1.37	4.01	2.73	1.88	2.78	3.09	2.35
$Ce(acac)_3$ (g)	0.03	0.04	0.05	0.04	0.05	0.06	0.02		
BPO (g)	0.14	0.10	0.06	0.17	0.11	0.08	0.12	0.14	0.10
ZrO_2−CeO_2 calcd (%)	13	17	21	14	21	27	52[a]	21	17
decomp onset temp (°C)	233	229	220	259	237	237	300	*b*	*b*

[a] Sample containing crystalline ZrO_2−CeO_2 powders. [b] Not measured.

Scheme 1

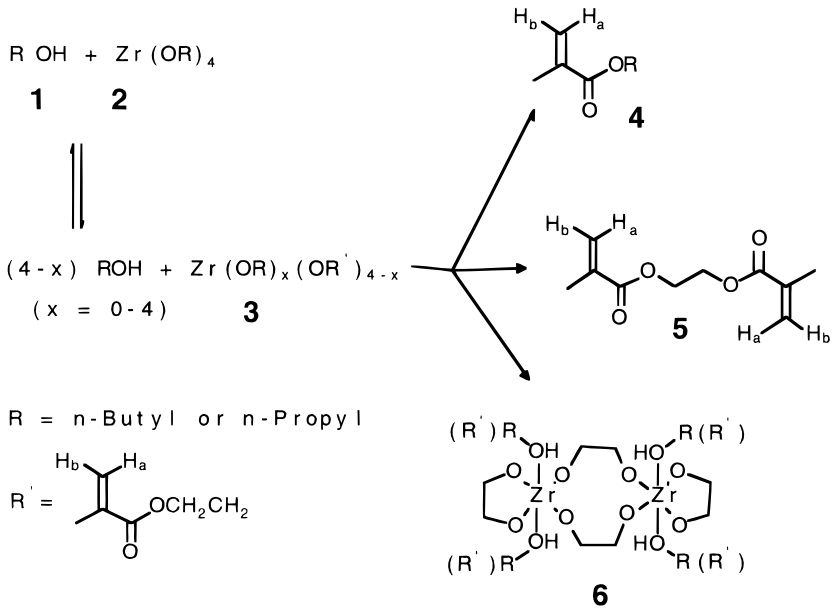

alkoxide with moisture in the air, and Zr−OR functionalities can react with the hydroxylic group of the HEMA organic monomers. Moreover, transesterification reactions can occur, producing propyl (or butyl) acrylate, ethylene glycol dimethylacrylate, and complex HEMA/Zr alkoxides. The occurrence of these reactions was investigated by nuclear magnetic resonance (NMR). In the second stage, the free radical polymerization of the vinyl moieties of HEMA can occur on heating the BPO-containing mixtures. Fourier transform infrared spectroscopy (FT-IR) and differential scanning calorimetry (DSC) techniques allowed us to assess the end of the polymerization.

Experimental Section

Preparation of Samples. All the preparations were made from commercially available reagents, used without further purification. Zirconium *n*-propoxide 70% in *n*-propanol or zirconium *n*-butoxide 80% in *n*-butenol were used as the source of the inorganic moieties. A number of copolymers were prepared, by varying the molar ratio r = [HEMA]/[Zr]. To obtain a ceria−zirconia−HEMA polymer, a reaction mixture of cerium(III) 2,4-pentanedionate, zirconium alkoxide ([Ce]/[Zr] = 0.01 molar ratio), and HEMA, containing 4 wt % BPO, were prepared, affording a pale brown solution. After vigorous stirring the solutions became homogeneous and could be cast into molds at room temperature, where the exothermic polymerization took place in a few minutes. The monolithic hybrid materials were cured for 2 h at 80 C. To prepare the zirconia−HEMA polymer, zirconium alkoxide and HEMA, with 4 wt % BPO, were mixed, affording a pale yellow solution. After vigorous stirring, the solution became homogeneous and could be cast into molds and inserted into an oven at 80 °C, where the polymerization and curing for 2 h took place, affording monolithic rods (1 cm in diameter and 10 cm long). The polymerization of each solution was also followed by DSC analysis.

The composition, thermogravimetrical features, molar ratio, and decomposition onset temperatures of the hybrid materials are listed in Table 1.

Synthesis of Ethylene Dimethacrylate (EDMA) (5 in Scheme 1). Solid K_2CO_3 (≈100 mg) was added to 500 μL of HEMA and the mixture stirred at room temperature for 90 min. The mixture was subjected to flash chromatography (Merck silica gel, hexane/ethyl acetate gradient) to give **5** (485 mg), identified by ^{1}H NMR.

Synthesis of Butyl Methacrylate (BMA) (4 in Scheme, R = *n*-Butyl). Solid K_2CO_3 (≈100 mg) was added to a solution of HEMA (500 μL) and 1-butanol (2 mL) in hexane (5 mL) and the mixture stirred at room temperature for 150 min. Purification of the mixture, as reported for the EDMA preparation, gives **4** (R = *n*-butyl, 406 mg) and **5** (125 mg), identified by ^{1}H NMR.

Synthesis of Propyl Methacrylate (PMA) (4 in Scheme, R = *n*-propyl). Solid K_2CO_3 (≈100 mg) was added to a solution of HEMA (500 μL) and 1-propanol (2 mL) in hexane (5 mL) and the mixture stirred at room temperature for 150 min. Purification of the mixture, as reported for the EDMA preparation, gives **4** (R = *n*-propyl, 346 mg) and **5** (118 mg), identified by ^{1}H NMR.

Characterization of Samples. Infrared spectra (FT-IR) were recorded using a FT-IR Bio-Rad FTS 165 instrument in the reflectance mode (unpolarized beam reflected).

The NMR spectra were recorded at 22 °C with a Varian XL-300 spectrometer in 5 mm o.d. sample tubes [δ values (ppm)

relative to internal Me_4Si (0.00 ppm)]. The ^1H NMR FIDs were acquired with 20 032 points, zero-filled to 65 536, and then processed. The ^{13}C NMR FIDs were acquired with 20 232 points, zero-filled to 65 536, weighted with an exponential function (1 Hz line broadening), and then processed. The samples were prepared on adding zirconium butoxide (30 μL, 80 wt % in butanol) or zirconium propoxide (30 μL, 70 wt % in propanol) and 40 or 50 μL of HEMA, respectively, to 600 μL of deuterated solvent ($CDCl_3$ or DMF-d_6).

DSC measurements were performed with a Mettler DSC 30 calorimeter in the range 0−150 °C (or 0−200 °C), with flushing nitrogen at 100 mL/min, by computer assistance with a built-in Graphware TA72 program. A sample of pure indium was used for calibration of temperature and enthalpy. The heat of polymerization was evaluated by integration of the exothermic peak developed in the range 50−110 °C by about 70 mg of fresh reactive mixture heated at 5 °C/min. Endothermic peaks, if any, were attributed to evaporation of volatile reagents and byproducts and were related to the percentage of mass loss after DSC scanning. The thermal stability of cured hybrid materials was evaluated from the onset point above 200 °C.

Electron impact mass spectra (El-MS, 70 eV) were continuously recorded and stored, with scans from 3 to 400 amu in steps of 0.9 s with a delay time of 0.1 s with a VGQMD1000 quadrupole mass spectrometer (Carlo Erba Instrument) as a detector and helium gas carrier.

High-pressure liquid chromatography (HPLC) was performed on a Merck LiChrospher Si-60 column, 5 μm, with UV detector at 250 nm.

Dynamical mechanical thermal analyses (DMTA) were performed on solid samples by using a PL-DMTA MkII instrument of Polymer Laboratories in a shear configuration. Disks of about 9 mm diameter and 2 mm thickness were measured at a frequency of 1 Hz, with a linear displacement of 0.016 mm along the diameter direction. Shear storage modulus (G'), loss modulus (G''), and loss factor (tan δ) were measured from 0 to 150 °C with a heating rate of 3 °C/min. The values of T_g were read off as the temperatures of the peak of the loss factor.

Results and Discussion

Different procedures were used in order to produce hybrid materials. The first approach involved a solution process, but a long drying stage followed gelation. The high shrinkage associated with this preparation led us to set up a procedure which did not involve adding a solvent.

$Zr(OR)_4$ and HEMA Systems. The inorganic precursor $Zr(OR)_4$, in the presence of HEMA, shows exchange of alkoxide groups[20] and affords a stiff gel at room temperature, attributable to the formation of the compound **6** (see Scheme 1).[21] This seems clear on the basis of the NMR results, which also suggest the existence of expected equilibrium reactions between the zirconium alkoxide and HEMA, with the formation of byproducts.[20] To understand which chemical reactions are involved, ^1H NMR and ^{13}C NMR spectra (in $CDCl_3$ and DMF-d_6) were recorded immediately after the mixing of the reagents and, subsequently, until gelation. The ^1H spectra of the $Zr(OPr^n)_4$/HEMA mixture are reported in Figure 1. The broad signals of the spectrum recorded after the mixing of the reagents suggest that the reagents **1** and **2** are involved in a fast exchange with species **3**, providing direct evidence that the organometallic compound incorporates the monomer (see Scheme 1). Afterward, the chemicals involved in the fast equilibrium (alcohols ⇔ alcoholates) slowly and partially change into ester compounds. In all of the spectra, a high-field, broad signal is present, which is attributable to exchangeable H (*H*OR of propanol and HEMA). In the top spectrum of Figure 1 appears also a triplet at about 3.13 ppm, which can be assigned to $HOCH_2$ groups engaged in H-bonding.

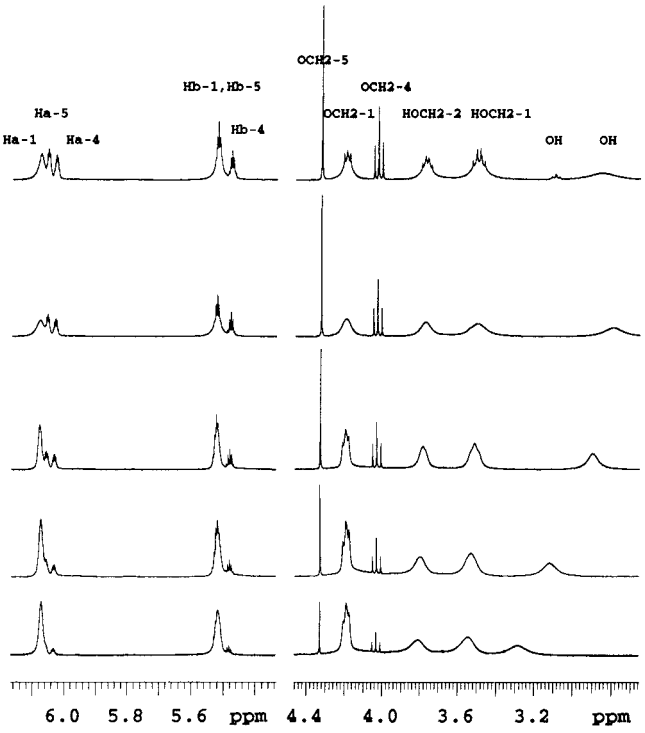

Figure 1. ^1H spectra of $Zr(OPr^n)_4$ (**2**) and HEMA (**1**) with r = 1: resonance of olephinic protons (left) and protons linked to oxygen-bearing carbon atoms (right) at increasing times after mixing (from the bottom, 10, 23, 64, 158, and 521 min respectively). Labels: H_a-**4**, H_b-**4**, and OCH_2-**4** refer to ester **4**; H_a-**5**, H_b-**5**, and OCH_2-**5** refer to ester **5**; H_a-**1** and H_b-**1** refer to HEMA (**1**); $HOCH_2$-**2** and $HOCH_2$-**1** refer to methylenic protons of **2** and **1** (see Scheme 1).

Moreover the NMR spectra suggest the presence of the esters **4** and **5**, obtained by transesterification reactions with the release of 1,2-ethanediol, where the latter is conjecturally involved in the formation of the species **6**.[21] Actually, other signals of species **6** are not detectable in the NMR spectra, because it forms a gel in the NMR tube, driving out a liquid phase containing **3**−**5**. The catalytic activity of zirconium ion can account for this pathway, even if other reaction routes cannot be definitely excluded.

To demonstrate the formation of esters **4** and **5**, they were synthesized and added to the $Zr(OPr^n)_4$/HEMA mixtures, thus modifying the ^1H spectra as shown in Figure 2. In fact, the middle spectrum, obtained by adding the ester **4** (R = *n*-propyl), shows an increase of OCH_2 (4.08 ppm) and $C{=}CH_2$ (5.48 and 6.02 ppm) signals, attributable to compound **4**. Analogously, the top spectrum, obtained by adding the ester **5**, shows an increase of $OCH_2{-}CH_2O$ (4.33 ppm) and $C{=}CH_2$ (5.53 and 6.07 ppm), resonances attributable to the compound **5**.

Similarly to the experiment reported by Wei et al.,[14] the material obtained from the sol−gel reactions of the

(20) Nabavi, M.; Doeuff, S.; Sanchez, C.; Livage, J. *J. Non-Cryst. Sol.* **1990**, *121*, 1.
(21) Chaibi, J.; Henry, M.; Zarrouk, H.; Gharbi, N.; Livage, J. *J. Non-Cryst. Solids* **1994**, *170*, 1.

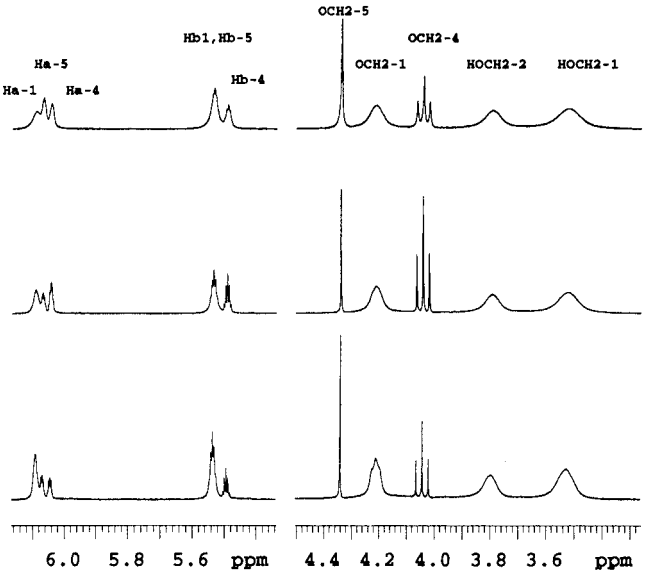

Figure 2. ^{1}H spectra of the mixture of $Zr(OPr^n)_4$ and HEMA with $r = 1$: resonance of olephinic protons (left) and proton linked to oxygen-bearing carbon (right) after 90 min (bottom), after addition of PMA (middle), and after further addition of EDMA (top). Labels: see Figure 1.

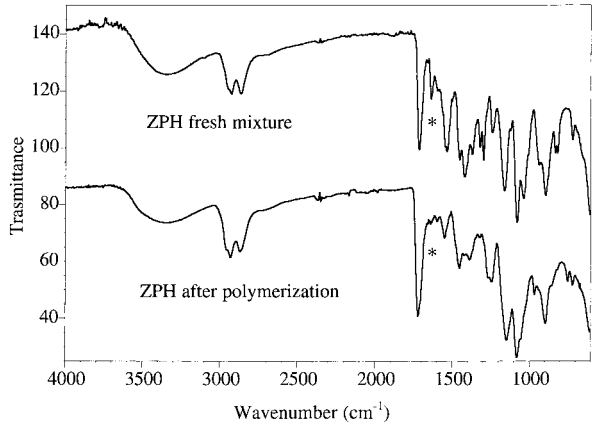

Figure 3. IR spectra of the sample ZPH as a fresh mixture (top) and after polymerization (bottom).

$Zr(OPr^n)_4$/HEMA ($r = 1$) mixture was ground and extracted exhaustively with THF using a Soxhlet apparatus. The HPLC analyses of the coelution of the THF extract with synthesized **4** and **5** indicate an approximate **5**/**4** molar ratio of 2/5 and the absence of free HEMA. The ^{1}H NMR analyses, not here discussed, also indicate that the **5**/**4** molar ratio increases with *r*.

Seemingly, the alkoxide group does not have a noticeable effect either on the overall rate of the process affording the hybrid material or on the amount of shrinkage. When solvent is present, syneresis accompanies the formation of the gel. Figure 3 (top) shows a typical IR spectrum, in which are present the peaks at 1720 and 1636 cm^{-1}, attributable to the stretching vibrations of the carbonyl bonds (C═O) and carbon−carbon double bonds (C═C), respectively, in the HEMA moiety.

The DSC curves of fresh mixtures of $Zr(OBu^n)_4$ and HEMA evidence a small exothermic effect, corresponding to the formation of the gel network, and a broad endothermic peak of evaporation (see Table 2). Irrespective of the HEMA/Zr molar ratio (*r*), the mass loss

Table 2. Temperatures and Δ*H* Corresponding to the Exothermic and Endothermic Peaks, along with the Mass Losses Recorded during the DSC Analyses (0−200 °C) of $Zr(OBu^n)_4$ and HEMA Systems at Different [HEMA]/[Zr] Molar Ratios (*r*)

	exothermic		endothermic		
r	*T* (°C)	Δ*H* (J/g)	*T* (°C)	Δ*H* (J/g)	mass loss (%)
4	60	11	137	220	63
2	63	10	120	201	65
1	59	3	114	181	60

Table 3. Temperatures and Δ*H* Corresponding to the Exothermic and Endothermic Peaks, along with the Mass Losses Recorded during the DSC Analyses (0−150 °C) of $Zr(OBu^n)_4$, HEMA, and BPO Systems at Different [HEMA]/[Zr] Molar Ratios (*r*)

	exothermic		endothermic		
r	*T* (°C)	Δ*H* (J/g)	*T* (°C)	Δ*H* (J/g)	mass loss (%)
4	79	132	123	70	30
2	74	71	116	107	40
1	65	29	119	129	51

of all the samples is about the same and pronounced, about 60%, because of the release of **4** and **5** and butanol, the species present in the liquid phase, as evidenced by the NMR and HPLC analyses. The final product is reasonably supposed to be a gel network of zirconium ions cross-linked by Zr−O−Zr and Zr−OCH_2-CH_2O−Zr bridges. The higher the *r*, the higher the number of OCH_2CH_2O residuals in the final gel structure.

$Zr(OR)_4$, HEMA, and BPO Systems. In the presence of benzoyl peroxide, the NMR experiments evidence that the reactions have a similar course at room temperature, with the main difference being the increase of $HOCH_2$−R groups involved in hydrogen bonds. Similarly to the previous system, the reaction batch is a mixture of unmodified alkoxides $Zr(OR)_4$, modified precursor $Zr(OR)_x(OR')_{4-x}$, and the byproducts as **4** and **5** of Scheme 1, the amount of which strictly depends on the time.

The DSC curves of the gelled mixtures show nothing but a large endothermic peak attributable to evaporation; no polymerization occurs even if the species **3**−**5** are polymerizable. A possible explanation of the absence of polymerization involves the formation of species **6** and its oligomeric derivatives, leading to a gel.[5,21] Owing to the increase of viscosity occurring after the gelation, the mobility of monomers and the propagation of the polymerization reaction are restricted.

On the contrary, the DSC analyses of the fresh mixtures show strong exothermic peaks attributable to the polymerization of vinyl groups (see Table 3). In the IR spectra of the samples heated to 150 °C during the DSC analyses, it is also apparent that the intensity of the C═C absorption band at 1636 cm^{-1} decreased significantly, indicating the occurrence of the vinyl polymerization. In Figure 3 (bottom) is shown an example of the IR spectrum of sample ZPH polymerized at 80 °C for 2 h.

Moreover, as reported in Table 3, all of the samples obtained from fresh mixtures show polymerization temperatures lower than pure HEMA (about 100 °C). This suggests that the role of the transition metal should be invoked to account for the low temperature of the BPO peroxy bond cleavage, forming radical

species. Furthermore, in Table 3 the values of the polymerization heat for the mixtures can be seen. These values are lower than those expected theoretically. In fact, in the solutions there is not free HEMA but species **3**, modified monomers **4** (BMA), and **5** (EDMA), for which the specific polymerization heats are presumably higher than the value measured for the pure HEMA (290 J/g). Hence, an incomplete conversion of the vinyl groups can be supposed, mainly because the heating promotes both the radical polymerization and the gelation. As discussed before, the gel traps a certain amount of monomers, not available for the polymer chain building up. In fact, each DSC curve shows the endothermic peak related to the evaporation of butanol, **4**, and **5**, which did not undergo polymerization. The mass losses increase from about 30 to 50% (see Table 3), with the decrease of *r*. Notwithstanding, the presence of species **3** in the reaction mixtures affords the formation of hybrid polymers based on zirconia−HEMA, containing inorganic−organic domains. The DSC analyses of mixtures prepared with $Zr(OPr^n)_4$ show similar trends.

Large monolithic pieces are obtained from the mixture, in polypropylene tubes after the heating at 80 °C, but they result in mechanically weak materials, because most of the HEMA has not polymerized. Extension of the curing time beyond 3 h was found to yield white particles of inorganic zirconia hydroxide, causing cracks inside the rods.

$Zr(OR)_4$, HEMA, Cerium(III) 2,4-Pentanedionate, and BPO Systems. In this type of system the presence of cerium(III) 2,4-pentanedionate ($Ce(acac)_3$) has a noticeable effect on the stability of the solution of $Zr(OR)_4$ and HEMA: it does not form a gel at room temperature over a long time period. Due to the ligand exchange between $Ce(acac)_3$ and $Zr(OR)_4$, the coordination sphere of the zirconium can be easy completed by acac groups.[2,22] These strong chelating ligands decrease the reactivity of the alkoxides and obtain a control of the transesterification. This reaction requires HEMA and a butoxy group (or another HEMA molecule) both complexing to the same zirconium atom before the release of 1,2-ethanediol, increasing the coordination sphere of zirconium. Anyway, a similar configuration and the modification of zirconium with 1,2-ethanediol are not achievable in the presence of bulky acac ligands, so that the transesterification is avoided. According to the NMR results, in these systems the HEMA monomer is linked to zirconium as species **3**, whereas the formation of the byproducts **4**, **5**, and 1,2-ethanediol is restricted to a negligeable amount.

Through a mild heating and a short curing stage, the polymerization occurs, affording monolithic, transparent, colored rods. For all of these samples, upon polymerization the strong reduction of the peak at 1636 cm^{-1} in the IR spectra is apparent. However, as previously reported for the preparation of organic−inorganic polymeric materials,[14,23] a small amount of vinyl groups do not react during the polymerization owing to the lack of mobility. The occurrence of the polymerization is also confirmed by the DSC curves,

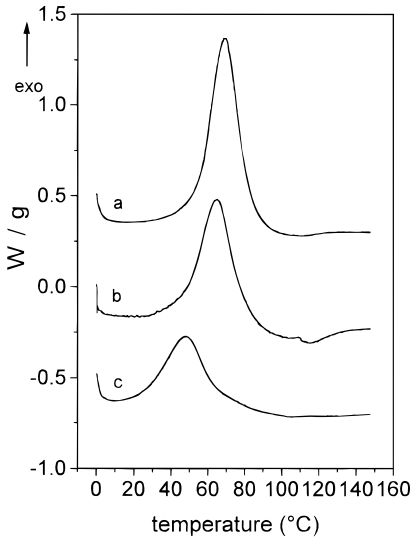

Figure 4. DSC analyses for the ZBH14 (a), ZBH12 (b), and ZBH11 (c) fresh mixtures.

Table 4. Temperatures and Δ*H* Corresponding to the Exothermic and Endothermic Peaks, along with the Mass Losses Recorded during the DSC Analyses (0−150 °C) of $Zr(OR)_4$, $Ce(acac)_3$, HEMA, and BPO Systems at Different [HEMA]/[Zr] Molar Ratios (*r*)

	exothermic		endothermic		mass
r	*T* (°C)	Δ*H* (J/g)	*T* (°C)	Δ*H* (J/g)	loss (%)
			R = Bu^n		
4	68	236	108	9	12
2	65	169	116	31	25
1	51	106	107	10	9
			R = Pr^n		
4	59	279			12
2	56	186	92	17	15
1	52	124	99	16	20

showing strong exothermic peaks (see Figure 4 and Table 4). Moreover, with respect to the homologues without cerium, the DSC analyses have highlighted lower mass losses up to 150 °C, higher polymerization heats, and lower polymerization temperatures.

In fact, the free radical reaction occurs when the vapor pressure of the volatile monomer is low enough to minimize evolution. The residual monomer can polymerize quantitatively and avoid the release of the other volatile species, such as butanol, so that the overall process of evaporation is reduced (Table 4).

As concerns the polymerization heat, Figure 5 compares the experimental value with that which the same quantity of free HEMA should give off theoretically, calculated from the experimental polymerization heat of pure HEMA (290 J/g), assuming a linear dependence on its weight percentage. A strong inverse correlation is observed between the polymerization heat and the alkoxide weight percentage. In particular, the polymerization heat of the hybrid materials always appeared greater than the corresponding theoretical value. This suggests that the monomer involved in the polymerization is not free HEMA but the species mainly present, namely the zirconium−HEMA complexes. These findings provide evidence that the achieved product is a hybrid material.

The catalytic effect of the metal ion in the polymerization reaction could be ascribed to the coordination of the BPO carbonyl groups to Zr^{4+}, affording an unstable

(22) Hoebbel, D.; Reinert, T.; Schmidt, H.; Arpac, E. *J. Sol-Gel Sci. Technol.* **1997**, *10*, 115.
(23) Ferracane, J. L.; Greener, E. H. *J. Dent. Res.* **1984**, *63*, 1093.

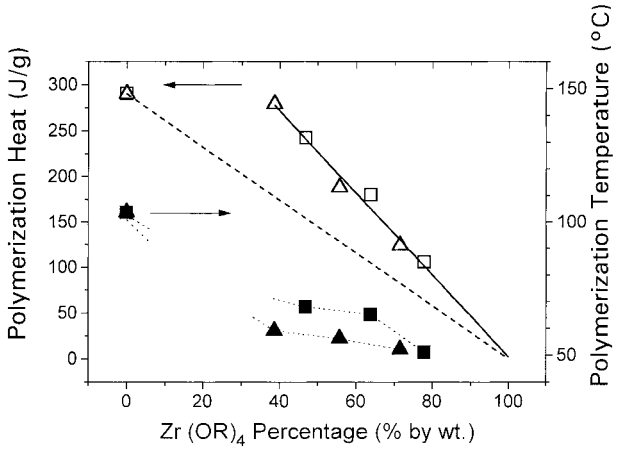

Figure 5. Polymerization heat (□, R = Bu^n; △, R = Pr^n) and polymerization temperatures (■, R = Bu^n, ▲, R = Pr^n) vs Zr-$(OR)_4$ wt % in the mixtures for $Zr(OR)_4$, HEMA, cerium(III) 2,4-pentanedionate, and BPO systems. The straight dotted line represents the theoretical values of polymerization heat, assuming that free HEMA polymerizes completely.

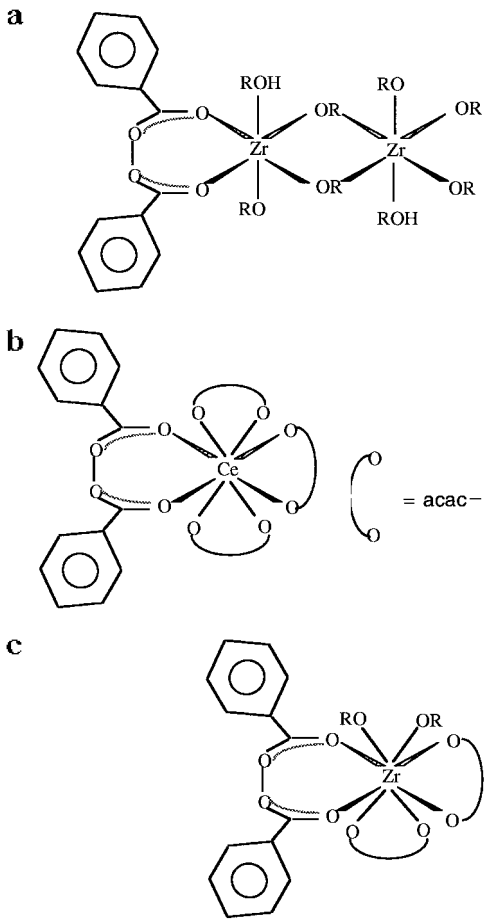

Figure 6. Hypothetical intermediates for catalyzed polymerization.

seven-membered ring, as depicted in Figure 6a. This intermediate develops into radical species after the peroxy bond breaking. According to this mechanism, an alkoxy group shorter than butoxide should reduce the steric hindrance around zirconium and increase the amount of intermediate complexes. In agreement with this hypothesis, the DSC analyses curves of the samples containing $Zr(OPr^n)_4$ showed a lower polymerization temperature, and also the preliminary experiments with

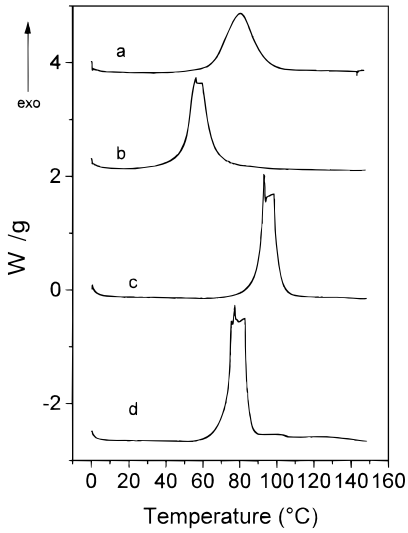

Figure 7. DSC curves of the ZPH14 (a), ZPH (b), HEMA (c), and HEMA with cerium(III) 2,4-pentanedionate (d) fresh mixtures containing the same BPO percentage with respect to the amount of HEMA.

$Zr(OEt)_4$ evidenced a further decrease. On the other hand, the catalytic effect of the zirconium appears more evident by observing, in Figure 5, the decrease of the polymerization temperature as the amount of $Zr(OBu^n)_4$ increases. The same trend is shown by the samples containing $Zr(OPr^n)_4$.

Moreover, when a catalytic amount of zirconium di-*n*-butoxide bis-2,4-pentanedionate was added to HEMA, a decrease of the polymerization temperature of about 10 °C and an increase of polymerization heat with respect pure HEMA were found. These results could be again explained by the chelating effect on the metal ion of BPO, with the formation of radicals at low temperature, and of 2,4-pentanedionate, which avoids transesterification. As a consequence, also the addition of pure 2,4-pentanedione (acacH), as much as [acacH]/[Zr] = 0.03, to the mixtures of $Zr(OBu^n)_4$, HEMA, and BPO not only inhibits the gel formation but also allows the quantitative polymerization of HEMA and the formation of transparent colorless rods.

Actually it is noteworthy that an autocatalytic polymerization occurs in about half an hour for all of the samples containing acac groups, provided the mold is tightly closed in order to avoid thermal exchange. As confirmed by the DSC curves, the polymerization starts at 25−30 °C (see Figure 4), so that the process could propagate, even at room temperature.

Moreover, in Figure 7d the DSC curve of the mixture of HEMA, BPO, and catalytic loadings of cerium(III) 2,4-pentanedionate can be seen. It shows that the polymerization occurs at lower temperature with respect pure HEMA containing the same amount of BPO. Since other experiments showed that no polymerization takes place when mixing HEMA and cerium(III) 2,4-pentanedionate only, the latter must react with BPO. Although Ce^{4+} is a well-known polymerization catalyst,[24] we presume that the key to the catalytic effect can be found in the complexation of the reduced form, Ce^{3+}. In fact, no evidence could be collected about the

(24) McDowall, D. J.; Gupta, B. S.; Stannet, V. T. *Prog. Polym. Sci.* **1984**, *10*, 1.

Table 5. Chemical Analysis of the Samples ZBH14 and ZBH11

	weight percent	
	ZBH14	ZBH11
C	50.2	40.1
H	8.2	7.1
Zr	10.3	19.0
Ce	0.12	0.24

hypothesis that Ce^{4+}, deriving from a redox reaction between Ce^{3+} and BPO, is the actual catalyst of polymerization. To more fully elucidate the role of cerium during the polymerization reaction, mixtures of HEMA containing BPO and different cerium compounds (e.g. $CeCl_3$, $Ce(OOCCH_3)_3$, and $Ce(OH)_4$) were prepared and analyzed by DSC as well. None of these mixtures showed a decrease of the polymerization temperature with respect to that of the pure HEMA. The lowering in the polymerization temperature is necessarily due to cerium(III) 2,4-pentanedionate, which may enlarge its coordination sphere by complexation.[25] Probably here BPO could chelate Ce^{3+}, forming an intermediate complex (Figure 6b), similar to zirconium.

Hence, Ce(III) 2,4-pentanedionate is double-acting in the production of this type of hybrid material, consisting of an organic network of poly-HEMA, linked to the inorganic zirconium ions. Microstructural analyses revealed the homogeneity of the materials, which show a glassy fracture surface, very similar to that of the pure zirconia gel. In general, these materials show a clear decomposition onset temperature (see Table 1), and despite the large shrinkage, most of the samples obtained from the mixtures without the solvent were crack-free after the decomposition.

The chemical analysis of the ZBH14 and ZBH11 gives the results in Table 5, which show that the first sample maintains the initial organic load almost unchanged, whereas the second one increases its inorganic character. The TG−MS measurements on the same samples could explain their different behavior. The whole mass loss of the sample ZBH11 is about 40 wt %, and it loses butanol already at room temperature because of reaction with air moisture. In fact the total ion curve (TIC) of this sample shows a strong peak at the boiling point of the butanol, the evolution of which is confirmed by the MS spectrum. At the same temperature, a small amount of BMA is detected too. A second evolution of the same species (butanol and BMA) is recorded at higher temperature (about 300 °C), as ensuing from different reaction mechanisms. The losses at temperatures above 300 °C could be mainly ascribed both to the depolymerization, giving off monomer as typically reported for methacrylate polymers,[26] and to the pyrolysis of organic residuals, leading to the evolution of CO and CO_2. An interesting result, inferred from the MS spectrum at high temperature, is the formation of aromatic species (benzene, toluene, xylene). This suggests a pyrolysis pattern in which the formation of those species implies the rearrangement reactions of the organic residuals, catalyzed by zirconium ion.[27] As

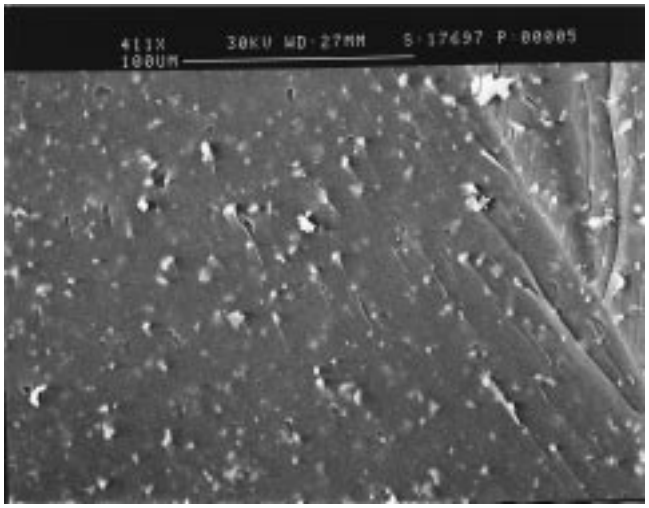

Figure 8. SEM micrograph of a fracture surface of the ZBHM hybrid material.

concerns the sample ZBH14, although the mass loss is greater (70 wt %), it appears more stable at low temperature. The evolution of parent alcohol is completed in a single loss at higher temperature, confirming the minor sensitivity of this sample to the moisture in the air, and the depolymerization and organic pyrolysis start above 300 °C. From these results it can be inferred that the decomposition onset temperature recorded by DSC should be ascribed to a shrinkage following the release of the volatile species, rather than to the decomposition of the polymeric chains.

The zirconia−ceria weight percentage has been varied between 10 and 50, but the inorganic content can be further increased by the mineral addition of crystalline powders. As an example, the morphology and the microstructural features of the ZBHM sample are shown in the SEM micrograph of Figure 8. Owing to the presence of the inert powder, this sample shows the best thermal behavior and a decomposition onset temperature above 300 °C.

DMTA Analyses. To get more information about the structure of these hybrid materials, further experiments were performed. Disks of $Zr(OBu^n)_4$, $Ce(acac)_3$, HEMA, and BPO systems with $r = 4$, as derived from both the procedures (solvent and solvent-free), were analyzed by DMTA in the shear mode. Figure 9a,b shows the results of the first and second scan of the dried and cured disks obtained from the solvent procedure. The presence of the glass transition temperature (T_g), confirming the formation of polymer chains, was deduced from the inflection of the storage modulus curve and from the corresponding peaks in the curves of the loss modulus and tan δ. The T_g value was about 80 °C in the first scan and 90 °C during the second one. However, all of the T_g values exhibited by the hybrid materials are lower than that of the pure poly-HEMA (100 °C).[28] G' at room temperature was 34 MPa, and increased up to 38 MPa in the second scan due to the thermal treatment. In the same time, G'' at room temperature decreases slightly from 1.1 to 0.9 MPa, as a consequence

(25) Cotton, F. A.; Wilkinson, G. *Advanced Inorganic Chemistry*; Interscience Publishers: John Wiley & Sons: New York, 1972.

(26) Kine, B. B.; Novak, R. W. in *Enc. Polym. Sci. Eng.*, 2nd ed.; Mark, H. F., Bikales, N. M., Overberger, C. G., Menges, G., Eds.; John Wiley & Sons: New York, 1985; p 265.

(27) Di Maggio, R.; Campostrini, R.; Guella, G. *Chem. Mater.* Submitted.

(28) Fambri, L.; Gavazza, C.; Stol, M.; Migliaresi, C. *Polymer* **1993**, *34*, 528.

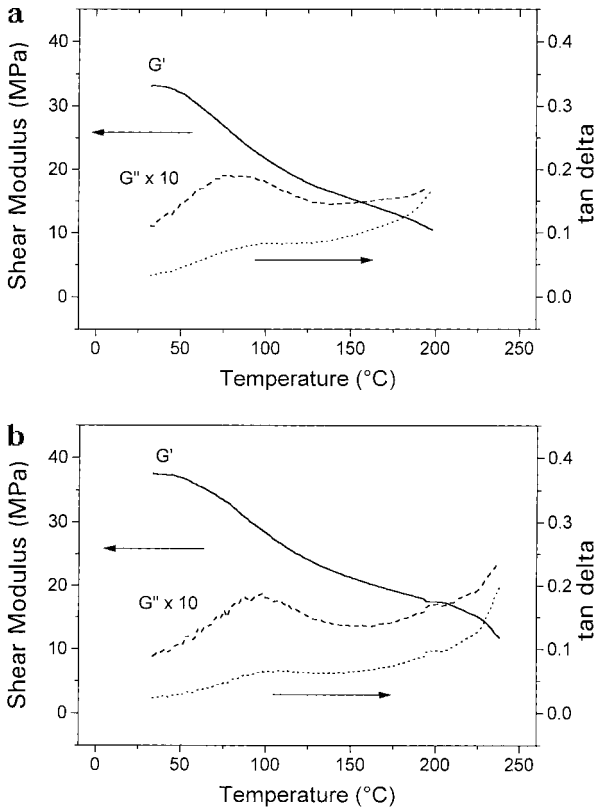

Figure 9. Shear storage modulus (G'), shear loss modulus (G''), and damping factor (tan δ) of the ZBH14 hybrid materials. The first scan was performed after drying and curing the disks (panel a), whereas panel b represents the second scan of the same sample.

of the progressive cross-linking and the decrease of the residual polymerization in the organic moiety. Both of these effects increase the rigidity and decrease the viscoelastic behavior of the system.

On the contrary, the hybrid materials obtained from the solvent-free procedure showed not only lower shrinkage and defect content but also higher storage moduli at room temperature (55 and 65 MPa in the first and second scan, respectively). The loss modulus curve showed a glass transition temperature in the range 40−70 °C, and G'' is, at room temperature, about 3 MPa, 3 times higher than the corresponding value of the material derived from the solvent procedure. In the latter case, a lower polymerization degree could account for the lower viscoelasticity of the overall system.

Independent of the composition, the solvent procedure evidenced its limit: generally, the samples crack during the DMTA tests. The higher the dilution, the lower the polymerization of the organic monomer and the higher the shrinkage. Thus, at the present only the stable hybrid materials obtained from solvent-free procedure were further analyzed by the DMTA technique and the results will be presented in a forthcoming paper.

Conclusions

The preparation and characterization of hybrid materials, derived from the mixtures of HEMA and zirconium alkoxides, are described. The formation of bonds between the organic and inorganic components has been established by ^{1}H and ^{13}C NMR experiments, during the reaction of the HEMA with the zirconium alkoxide. These results confirm the feasibility of creating the hybrid polymers, starting from polymerizable organic monomer and metal alkoxides.

The main results can be briefly summarized by the following points: (a) $Zr(OR)_4$ and HEMA always form a stiff gel; (b) $Zr(OR)_4$, HEMA, and BPO give a weak hybrid polymer, when the mixture is heated before the gelation; (c) the gelation has to be avoided, because of the relative increase of viscosity that reduces the polymerization; (d) crack-free rods have been obtained, in polypropylene molds with heating at 80 °C, from the solutions of HEMA (containing 4 wt % BPO), $Zr(OR)_4$, and cerium(III) 2,4-pentanedionate (or 2,4-pentanedione); (e) both $Zr(OR)_4$ and cerium(III) 2,4-pentanedionate expand their coordination sphere via chelating BPO molecules and catalyze the cleavage of O−O bonds and the formation of radicals at room temperature; (f) the acac group enables the zirconium ion to catalyze the polymerization, avoiding the transesterification reactions of HEMA.

The zirconia-based polymers are not affected by a noticeable shrinkage, since they can be obtained without any solvent and with a very small amount of byproducts. Consequently, they can be easy shaped in large monoliths. Furthermore, the inorganic content could be increased by introducing powder or fibers, so that the microstructure of the hybrid composite can be tailored according to the desired properties. Although these new zirconia-based polymers do not yet match all the requirements for practical uses, they could be used as protective coatings or optical or structural materials for temperatures up to 300 °C.

Acknowledgment. The authors thank Dr. Renzo Campostrini for TG−MS measurements and for the helpful discussion.

CM970694J